Feature Indexing in a Database of Digitized X-rays

L. Rodney Long*, George R. Thoma

National Library of Medicine, Bethesda, MD 20894

ABSTRACT

We have the goal of developing computer algorithms for indexing a collection of digitized x-ray images for biomedical features important to researchers in the fields of osteoarthritis and vertebral morphometry. This indexing requires the segmentation of the image contents, identification of relevant anatomy in the segmented images, and classification of the identified anatomy into categories by which the image contents may be indexed. An example of the indexing detail that we have as a goal is, "disc space narrowing at vertebra location C5-6". This is a work in progress, with much current activity still in the segmentation step. We approach this segmentation as a hierarchical procedure with the distinctive regions of the image, including the general spine region, first being segmented at a gross level of detail, followed by a finer level segmentation of the spine region into individual vertebrae. In this paper we report on work done toward the gross level segmentation and also describe the image-level characteristics of one of the features targeted for the final indexing step.

Keywords: digitized x-ray, segmentation, image processing, multimedia database, morphometry, osteoarthritis

1. INTRODUCTION

At the Lister Hill National Center for Biomedical Communications, a research and development division of the National Library of Medicine, we are developing a prototype multimedia database system to provide access to biomedical databases over the World Wide Web. This *WebMIRS (Web-based Medical Information Retrieval System)* will allow access to databases containing text and images and will allow database query by standard SQL, by image content, or by a combination of the two. The WebMIRS results screen is illustrated in Figure 1. The system is currently undergoing beta testing and is capable of retrieving text and associated cervical spine and lumbar spine x-ray images. However, except for image display, the current version is very similar to many other databases that are text-only: no image content information, such as dimension measures of specific anatomy, are currently available in the database; further, all queries are made with GUI-assisted standard SQL. No query by image example is currently possible. As work toward building these more advanced capabilities, we are addressing fundamental problems in the required image processing and pattern classification.

Current WebMIRS operation. When the current WebMIRS system is used, the user manipulates GUI tools to create a query such as, "Search for all records for people over the age of 60 who reported chronic back pain. Return the age, race, sex, and age at pain onset for these people." In response, the system returns a display of values for these four fields for all matching records, plus a display of the associated x-ray images.

Future WebMIRS operation. A future WebMIRS system is envisioned to have additional capabilities to support use such as the following:

Example 1: "Search for all records for people over the age of 60 who reported chronic back pain. Return the age, race, sex, age at pain onset, and ratio of anterior/posterior vertebral heights for the L4 vertebra."

Example 2: "Search for all records for people over the age of 60 who reported chronic back pain and who have an *L4 vertebra with shape resembling this one*. Return the age, race, sex, age at pain onset, and ratio of anterior/posterior vertebral heights for the L4 vertebra."

Realization of a system capable of carrying out the queries in examples 1 and 2 imposes different requirements. In example 1, the query is conventional; the data is simply text in relational tables. However, the cost practicalities in time and money of acquiring this data by the manual labor of medical experts are likely to prevent the data from being acquired this way. The

* Correspondence: Email: long@nlm.nih.gov, thoma@nlm.nih.gov

implication is that only by means of an automated or sufficiently cost-effective computer-assisted system will the data be successfully acquired. Hence, even to populate our RDBMS tables with this type of data, research into algorithms to segment and identify anatomy and derive measurements meaningful to the end user are needed.

In example 2, the query itself is non-conventional. The system is required to accept as input not just SQL, but an image in addition. The database tables contain *feature descriptors* for each image in the database. Now, the program has an additional requirement for a record to match the input query: the feature descriptors for the record being compared must satisfy a similarity requirement relative to the input image. For an example 2 system to become operational, basic problems in segmenting and derivation of feature descriptors must be solved in order to populate the RDBMS tables, plus the system must be enabled to accept a fundamentally different type of query; in addition, the system must incorporate a concept of similarity measurement for judging the degree to which an image in the database resembles an input image.

Our eventual goal is to have a system that will support not only example 1 but also example 2 queries. Toward this goal we are pursuing research into image processing techniques that will support the hierarchical segmentation of the images, first into anatomically-related regions at a level of gross detail, then a fine level segmentation of the spine area into individual vertebrae. This segmentation stage will be followed by a stage of identification of the anatomy within the spine by specific vertebra number, i.e. for the cervical spine, an individual vertebra will be identified as one of C1 through C7. Finally, the features of interest within the segmented, labeled spine anatomy will be classified. For example, the disc spacing for each pair of vertebrae will be classified as "normal" or "abnormal": a result might be, "C5-6 disc spacing is abnormal". This work is in progress: in this paper we report on results obtained for the gross level segmentation of the images, describe the technical detail of the overall approach, and illustrate the image level characteristics of one of the features of interest for the classification of the anatomy by features of interest (i.e. the "indexing").

2. PROBLEM

2.1 General system problem

To the best of our knowledge, no general solution to the problem of creating an effective automated system for the extraction of such biomedical information as we have described for large collections of digitized cervical spine and lumbar spine x-rays, or for extracting similar biomedical information from comparable image collections, has been reported in the technical literature. Results that have been reported include the development of Active Shape Model (ASM) algorithms requiring some human interaction to segment vertebral boundaries in DXA lumbar spine images[1], the implementation of Active Contour models to segment lumbar spine vertebrae[2], again with some apparent human interaction, and preliminary results[3] indicating potentially significant segmentation for part of the cervical spine, using Active Shape models, again with human interaction.

2.2 Specific feature indexing problem: anterior osteophytes of the cervical spine

An osteophyte is defined as "a bony outgrowth or protuberance"[4]. We are concerned with osteophytes on the front, or anterior of the cervical spine in our lateral view x-rays. (Posterior osteophytes have been judged by expert consensus to not be sufficiently observable in these images.) One important classification problem to solve is, given a cervical spine image, classify it as normal or abnormal for the presence of anterior osteophytes (AO). Tools and data available for the classification include (1) custom-written and off-the-shelf image processing algorithms for the segmentation of the vertebrae using deformable template models and (2) the results of manual expert classification for anterior osteophytes for 275 cervical spine images. The related query by image example problem is to find images in the database that resemble an input image *with respect to anterior osteophytes*. Hence, a nuance to the query by example method becomes apparent: when we do a query by example, merely searching for images "like" the input may not be sufficient, but, rather, we may need to qualify the query further by specifying in what way the input and the searched images are to be compared for similarity. Analogs to this type of qualification of query by example are found in some of the existing database products that allow query by example: these qualifications are usually of a global nature, however, and allow the user to weight the global characteristics "shape", "color", or "texture" differentially when comparing the input and searched images. What we need to do, in contrast, is to qualify the search by shape in a particular region of interest. In this paper we illustrate this problem for AO classification.

3. APPROACH

3.1 General system approach

We approach the general system concept in four steps.

(1) Gross-level image analysis. We include in this step general approaches intended to identify the region of interest containing the spine, including approaches that might not be considered segmentation in a strict sense, in that all of the pixels within the identified region do not necessarily share graylevel/connectedness characteristics. An example is using image data to place an anatomy-based coordinate system that will provide a reference frame for locating the spine axis and orientation. We have previously reported[5] on work that took such an approach; unfortunately, this approach depended heavily on having images with strong contrast both in the back of the skull and in the jaw area, and has a high failure rate when that contrast is lacking. A second approach is reported by Zamora[6]. In this paper we describe a third approach based upon the use of expected graylevel values for the main image regions in blurred, reduced resolution versions of the cervical spine images to find the centers of gravity of concentrated bright grayscale regions that correspond approximately to the skull and shoulder, and the center of gravity that corresponds approximately to the background region behind the skull. We present the results of using four different methods to classify these image "landmarks", and show work in progress toward the use of these landmarks for obtaining a first approximation of spine position and orientation. This position/orientation is expected to be used in future work for the placement of a spine template for accurately locating the spine region by a deformable template method, such as ASM. Once the spine region is located, the individual vertebrae are expected to be segmented by also using a deformable template method.

(2) Fine level image segmentation. To date, the most effective segmentation techniques that we have applied to these images have been in the use of deformable templates generated from sampling boundaries of individual vertebrae in sets of sample images. Most of this work has been in the use of Active Shape Modeling (ASM) and has been mainly applied to the cervical spine images. ASM requires the construction of (1) a shape model, created from statistically sampling boundary points of the desired shapes in a number of images; (2) a grayscale model that represents, for each boundary point, the expected statistics of the grayscale values in the neighborhood of that point. The grayscale model, like the shape model, is created from sampling actual values in a subset of the images. We have reported[3] preliminary results, and a more extensive test and validation process is currently underway. In these preliminary tests, visually good matches to known "truth" boundaries are observed in some cases, while a number of problem cases are also observed, including gross level nonconvergence in some cases. The problem causes and possible algorithm improvements are being worked at the current time. One problem observed early in the testing process was the need for good initial conditions (position, orientation, and scale) for the input shape model. This, in fact, was the driving force for the first step in our image analysis/segmentation approach: the need to first identify the region of interest for the spine, before applying ASM to segment the individual vertebrae in the spine.

(3) Identification of anatomy in the finely segmented image. An outstanding problem that we have not addressed to date is the identification of the anatomy within the finely segmented image. By this we mean the correct anatomical labeling of the specific vertebrae, such as "C1", "C2", etc. for the cervical spine. It is expected that the prominent image features in the fine segmentation that will play a significant role in this identification will include the spinous processes on the back of the spine at each of the vertebrae, and the usually-dark spaces between vertebrae.

(4) Feature classification (indexing). To date almost all of our classification work has concentrated on the feature of anterior osteophytes, for the reason that we have the most expertly classified examples of this feature. We address the progress of this work below.

3.2 Specific feature indexing approach: anterior osteophytes of the cervical spine

Our approach to the AO classification problem for these images consists of steps to (1) segment, (2) identify, and, finally, (3) to classify the vertebrae as normal/abnormal for AO. It is convenient to separate the "identify" step, by which we mean the labeling of the anatomy by its proper anatomical name, such as "C2", "C3", etc., from the "classify" step of judging the anatomy to be normal or abnormal for AO. For segmentation of the vertebrae, we are investigating several techniques within the general category of deformable templates. Most work to date has been done using the specific method of Active Shape Modeling (ASM). Accurate labeling of specific vertebrae is expected to be achievable as a result of building ASM models sufficiently complex to model the entire cervical spine, including features that typically delimit one vertebral boundary from

the that of the adjacent vertebra, such as the visually darker spacing between vertebrae and the spinous processes--prominent bony projections at the back of the spine for each vertebra. Finding successful methods of classifying the segmented, labeled vertebrae as normal/abnormal for AO is expected to require the investigation of several alternative methods. One method being studied is dual ASM segmentation of the vertebrae. In this method two models of the vertebrae are constructed. In the first model, (the "normal model"), we use only shape data from vertebrae that are known a priori to be normal for AO. In the second model (the "general model"), we use shape data from vertebrae that are known a priori normal for AO as well as vertebrae known a priori to be abnormal for AO. The idea is then, given an image with vertebrae to be classified, to fit both models to the image: for normal vertebrae, the two fits are expected to each approximately fit to the vertebral boundaries; for abnormal vertebrae, the general model is expected to fit, but the normal model is expected to converge to boundaries that omit the AO regions. The differences between these boundaries, as measured by curvature or length differences, for example, are potential discriminators for normal/abnormal classification of the vertebrae.

4. RESULTS

4.1 Gross level image analysis

A hierarchical approach to the analysis of these images begins with the identification of the regions corresponding to gross-level classifications. These classifications usually correspond to regions containing specific anatomy, but may be may also be regions identified purely on the basis of image characteristics, irrespective of the anatomical content. The significance of this level of analysis is that it should lead to a subsequent finer-grained result that approaches the goal of segmenting and identifying the vertebral anatomy and classifying the identified anatomy by the conditions of interest to us.

A hierarchy of analysis/segmentation that can hypothetically lead to the necessary segmentation of the vertebral regions is as follows: (1) identify basic orientation marks in the image; (2) use this basic orientation to initialize a segmentation of the general spine region; and, finally, (3) apply a segmentation method to the spine regions to segment the individual vertebrae. We have obtained results for (1) in automatically identifying landmarks for the near-skull region (as explained below), shoulder, and back-of-skull background (subsequently, just "background"), that appear reliable and promising for a subsequent step in spine region location. Those results are presented here.

At full spatial resolution, the cervical spine images exhibit a variability of image characteristics that is sufficient to significantly complicate analysis and segmentation of the contents. The most successful approaches that we have used require statistical or integrative techniques, or similar techniques that analyze the image contents by grouping pixels as regions, lines or curves, rather than individual points. An alternative approach is to begin the image analysis at a lower spatial resolution version of the image, produced by blurring and subsampling the original.

As the resolution of the cervical spine image decreases, the visual distinctions among the individual vertebrae are lost, as well as the spinous process anatomy at the back of the vertebrae, and all distinctive anatomical features within the skull area (teeth, sinus area, orbits of the eyes, etc.). At a very low resolution the predominant visual features of the cervical spine images are the bright spots in the image corresponding to the approximate skull and shoulder regions, and the distinctively dark region corresponding to the background behind the skull. As shown below, it is possible to segment these regions in a very low resolution version of the image, and to map from the centers of gravity of these regions to points in the full resolution image that correspond to landmarks in the near skull, shoulder and background regions in a reliable manner. These landmarks can then (presumably) be used to refine knowledge of the image anatomy in the full resolution image.

The algorithm that we have developed has the following steps, applied to an input image I of size 1462x1755 that has grayscale values normalized to lie between 0 and 1, corresponding to the minimum (maximum) grayscale value in the original image:

(1) B=G(I). Produce the blurred image B by filtering the input image I so that the pixels remaining after subsequent subsampling represent the grayscale characteristics of regions, rather than individual pixels, in the original image. For the filtering, we experimented with Gaussian filters G with a variety of parameters (filter size and sigma) by viewing the filtered images and noting whether the image had been largely reduced to the grayscale blob level, and chose a 100x100 filter with sigma of 100 to produce the severe blurring that we desired.
(2) SB=S(B). Produce the subsampled blurred image SB by using a subsampling process S on the blurred image B to reduce it in spatial dimensions to a size easy to analyze. One of the areas that we wanted to explore was, whether significant information could be obtained from very low-resolution versions of the images. With this motivation, we

used a subsampling factor of 2**8, so that the SB matrix is only of size 6x7, (as compared to the original image size of 1462x1755). Figures 2a and 2b show an example of an original image I and the resulted subsampled blurred image SB. In Figure 2b the two bright regions corresponding to skull and shoulder, and the dark background region behind the skull, can be observed.

(3) Identify the regions of interest rs1, rs2, and rbg in the subsampled blurred SB image, and compute landmarks within each of these regions. The regions rs1 and rs2 correspond to the two brightest blobs in SB, which we expect to correspond to the skull and shoulder regions. At this step we do not determine specifically which of the rs1 and rs2 regions is skull and which is shoulder. The region rbg corresponds to the dark image background behind and, in some images, on top of the skull. The identification of rs1 is accomplished as follows: (a) find the brightest grayscale value gb1 in the image SB; (b) using gb1 as a seed, grow a region containing gb1 by iteratively examining the 8-neighbors of pixels already in the region, and adding to the region any of these 8-neighbors having a grayscale value within a tolerance of gb1; the resulting connected region is rs1. The region rs2 is similarly found by finding the second brightest grayscale value gb2 in SB that lies in a region disjoint from rs1 (i.e. no 8-neighbors of rs1 boundary pixels lie in this region). Just as for rs1, the gb2 pixel is used to seed a region-growing operation that results in an 8-connected region of pixels rs2 that have grayscale values within a tolerance. The tolerances used to define connectivity of rs1 and rs2 were found experimentally: for rs1, the tolerance gb1-0.05*dr was used, and for rs2, the tolerance was gb2-0.05*dr, where dr is the dynamic range (max – min grayscale value) in the image SB. While determining useful tolerance values that hold across a range of images can be at best problematic in the full resolution images, we were able to determine, with relatively few trials of varying the tolerance values and viewing the resulting connected regions, that the above values result in connected regions that satisfactorily correspond to skull and shoulder. The background region rbg was determined by finding all pixels with grayscale value below a tolerance empirically determined by visual checks to produce satisfactory connected background regions across a range of images. (An absolute grayscale tolerance of 0.1 was used.) For each of the regions rs1, rs2, and rbg the corresponding centers of gravity cg1, cg2, and cbg were computed as landmarks.

(4) Classify the landmarks cg1 and cg2 as corresponding to approximate skull or shoulder regions. These landmarks were classified using four different methods. For each method the landmarks were labeled “SK” or “SH”, the labels were displayed at their corresponding (x,y) coordinates on the full resolution image, and the resulting labeled images were viewed. The background landmarks were also labeled “BK” and similarly displayed on these images. As each image was displayed we made a judgment as to the acceptability of the labeling. We considered a label “acceptable” if it clearly lay within the boundaries of the corresponding region on the full resolution image; we also considered a skull or shoulder label acceptable if the resulting skull-shoulder line segment lay reasonably close in position and orientation to the spine, so that it appeared to be sufficiently accurate to position and orient a spine region template for initializing a search for the spine region. The last criterion is subjective: the real validation of the labeling algorithm comes in the application of the results to the problem of locating the spine region. Figures 3a-c show examples of the labeling. Figure 3c illustrates a case of the “SK” landmark being placed off the skull region, but we still judged its placement acceptable for getting an approximate spine position and orientation by using the line passing through “SH” and “SK” as a reference, along with the knowledge of the placement of the background landmark “BK”. The first method used to classify the cg1 and cg2 landmarks is based on the observation that, for many full resolution images, the brighter pixels occur in the shoulder region. The second and third methods are based on the observation that in the full resolution images, the grayscale variance in the shoulder region is almost always low as compared to the skull grayscale variance. (Of course, in these tests, we are operating on very low-resolution images where the bright and dark pixels lying near object boundaries in the full resolution images have been smeared together.) The four methods used to classify cg1 and cg2 were as follows: (a) consider the brighter point of cg1, cg2 to be shoulder; (b) consider the point of cg1, cg2 with smaller grayscale variance in neighboring SB pixels to be shoulder; (c) each pixel in the image SB corresponds to a set of four pixels in the next highest resolution image (increased by a factor of 2 in x and y); map the SB regions rs1 and rs2 (which have centers of gravity cg1 and cg2, respectively) into the corresponding regions in the next higher resolution image; find the variance of each of these sets of pixels, and consider cg1 to be shoulder if the region corresponding to rs1 in the higher resolution image has the smaller grayscale variance, as compared to the variance of the region corresponding to rs2; else consider cg2 to be shoulder; (d) for each image, use the background region rbg to determine the “background corner”: the image corner closest to the background region; once the background corner is found, determine the “shoulder corner” of the image: the image corner expected to be closest to the shoulder region; finally, consider cg1 to be shoulder if it lies closest to the shoulder corner; else, consider cg2 to be shoulder.

Results of the automatic landmarking are shown in Table 1 for a set of 48 cervical spine images, and show that the classifications obtained by methods (a) and (d) yielded the identical results of 46 acceptable skull classifications and 48 acceptable shoulder classifications. Method (c) yielded 46 acceptable skull classifications and 47 acceptable shoulder

classifications. Method (b) relies on measuring the variance of the image SB in a 3x3 region centered at the candidate skull (shoulder) point, and the relatively poor performance of this method is not surprising, considering the severe blurring and subsampling used to produce SB. What is somewhat surprising is that, as shown by the performance of method (c), sufficient variance information is preserved in the next highest resolution image (of size only 12x14) to discriminate between skull and shoulder. It should be noted that methods (a) relies on comparing the differences between grayscale values; in some cases the differences between these values may be quite small. A similar comment may be made about the comparison of the variances in method (c). This suggests that in a larger test set, some failures may occur with these methods due to outlying cases where the skull grayscale (variance) is in fact greater than (less than) the shoulder grayscale (variance) in the low resolution images. Method (d), however, only relies on the suppositions that we can properly classify the background behind the skull, that we can identify the corresponding image corner closest to this background region, and, using this information, that we can identify the image corner where the shoulder is expected to lie. The shoulder point is then classified as the candidate point closest in Euclidean distance to this "shoulder corner" of the image. In all of the observed cases, the background region, background corner, and shoulder corner were reliably identified, and the differences in the Euclidean distance between each candidate point and the shoulder corner are much larger than the differences used to discriminate between the candidate points in methods (a) and (c). Hence, we might expect method (d) to prove to be the most reliable method of classifying the landmarks. The two failure cases in skull labelling for methods (a), (c) and (d) were for the same two images. Both of these images show strong leakage of light along the bottom border of the original x-ray film, which in each case results in one of the candidate landmarks which should have been placed in the skull region, being placed along the bottom border. The fact that method (a) was able to correctly label the shoulder landmark in both of these problem images, and that method (c) correctly labeled the shoulder landmark in one of these images, can be attributed to chance, since only method (d) has a rational basis for identifying the shoulder landmark in such a case. The brightness and size of these borders suggest that a method to automatically detect and remove them should be achievable and straightforward. One of these failure cases is shown in Figure 4a-b, where Figure 4a shows the labeling obtained when the classification method (c) was used, and Figure 4b shows the labeling when method (d) was used. In each case, there is no acceptably placed skull landmark, due to the influence of the bright border region. Method (d) however is still able to properly label one of the landmarks as "SH" (shoulder) since method (d) only relies on finding the landmark closest to the "shoulder corner" of the image.

Figure 5 illustrates the next step in the use of the gross level image analysis: the use of the SH, SK, and BG landmarks to find an approximate spine axis in the full resolution images. This is work in progress and is illustrated by Figure 5, where the SH-SK line segment is taken as an approximation to the spine axis. The edge points of the skull and shoulder that are intersected by the line segment were found by analyzing characteristics of the smoothed grayscale derivatives of the image along SH-SK in an automated algorithm. Performance testing and refinement of this algorithm are continuing; this is expected to lead to the use of the algorithm for the automated placement of a spine region template near enough to the spine region so that an iterative procedure such as ASM can effectively and accurately locate the spine.

4.2 Work toward indexing the images for AO

Figure 6 shows four images taken from a digital atlas of the cervical and lumbar spine that we developed and have described in previous work[7]. These images contain instances of anterior osteophytes (AO) as progressively severe levels from left to right, with the leftmost image having Grade 0 (normal spine) and the rightmost having Grade 3 (the most severe) osteophytes. The presence of AO in the images becomes noticeable in the cropped spine regions shown in Figure 7, where the Grade 2 and Grade 3 deformity in shape of the vertebrae at the bottom anterior corner is especially visible. Figures 8a-d show the same images as Figure 7, but in the form of surface plots viewed from a 90 degree elevation (directly overhead), with hand-drawn boundaries of the vertebrae and of other tissue boundaries visible in the cropped images. The problem of classifying the vertebrae as normal or abnormal for AO can be considered to be the problem of distinguishing among shapes such as those represented by Figures 8a-d, or at the least, a collapsed version of such a grading where, for example, Grades 0-1 might be classed as "normal" and Grades 2-3 as "abnormal".

This classification (or "indexing") problem for AO is a work in progress. Besides the 4-grade images contained in our atlas, we have acquired a reference data set of 275 cervical spine vertebrae that contains medical expert classifications of the vertebrae as "normal" or "abnormal" (2 grades) for AO. This data set was acquired for subjects aged 60 years and older, where the incidence of AO is relatively high. Table 2 gives a breakdown in the occurrence of AO for a sample of 75 of these images. In Table 2, VID = vertebral i.d., where, for example, "2" refers to vertebra C2; N = number of vertebrae with ID of VID that are visible in the 75 images; NU = number of vertebrae with only upper AO identified; NL = number of vertebrae with only lower AO identified; and NB = number of vertebrae with both upper and lower AO identified. For example, in the

sample of 75 images, there were 73 instances of C4 classifications (VID = 4); of these, 2 had AO on the upper vertebral corner only, 19 had AO on the lower vertebral corner only, and 9 had AO on both the upper and lower vertebral corners, for a total of 30 C4 vertebral abnormal for AO (and 43 normal for AO). This data was acquired under supervision of a board-certified radiologist, and provides a rich source of data both for model building and for testing the performance of our classification.

We have created MATLAB software functions to assist in the collection of shape data for the vertebrae, and have built ASM models that we have used for preliminary segmentation work, using commercial ASM software available as a MATLAB toolkit. Most of our work to date has modeled one or two vertebrae in the cervical spine and has only included vertebrae normal for AO. The results of this work[3] suggest that successful boundary segmentation may be achievable by the ASM method or related deformable template methods for a significant subset of our images. We are currently generalizing our model to include the cases of abnormal AO, modeling more vertebrae, extending the work to the vertebral labeling and classification steps, and investigating alternative deformable template segmentation methods.

5. CONCLUSION

Automating image analysis for digitized x-ray images of the spine for extraction of information related to osteoarthritis is still at an early stage. Effective algorithms will eventually need to include components for image segmentation, identification of segmented anatomy, and classification of the anatomy with respect to features of interest. In our work the most promising techniques for vertebral segmentation are in the area of deformable templates; in particular, the use of ASM algorithms has produced the most promising results. The application of these algorithms to segment the spine vertebrae require knowledge of the gross level image structure for the purpose of initializing the search for the fine level structure. In this paper we have shown that landmarks for approximate skull, shoulder, and background regions were obtainable on a set of 46 of 48 cervical spine images with an automated technique that analyzes the graylevel values in a highly blurred and subsampled version of the original image. We have also illustrated how these results may potentially be used as a reference for placing a spine template near the actual spine region. Further work is required to validate the concept of using the landmarks we have obtained to position such a template for the purpose of initializing an effective search for the spine region (by ASM or other deformable template methods). Being able to determine the spine region in this manner would then make possible the initialization of a search for individual vertebrae boundaries within the spine region. We have also illustrated the shape characteristics of one of the features of interest (anterior osteophytes) for which we want to index the images.

ACKNOWLEDGEMENT

The authors would like to acknowledge the work of Dr. Matthew Freedman, M.D. and Dr. Ben Lo of Georgetown University in providing significant biomedical and quantitative data from 600 digitized x-ray images for the continuing research into developing effective image processing techniques for the automated image analysis for biomedical applications.

REFERENCES

1. Smyth PP, Taylor CJ, Adams JE. Vertebral shape: automatic measurements with active shape models. Radiology, May 1999, vol. 211, no. 2, pp. 571-578.
2. Gardner JC, Heyano SL, Yaffe LG, von Ingersleben G, Chesnut III CH. A semi-automated computerized system for fracture assessment of spinal x-ray films. Proceedings of SPIE Medical Imaging 1996: Image Processing, Vol. 2710, Newport Beach, CA, February 12-15, 1996, pp. 996-1008.
3. Long LR, Thoma GR. Use of shape models to search digitized spine x-rays. Proceedings of IEEE Computer Based Medical Systems 2000, Houston, TX, June 23-24, 2000, pp. 255-260.
4. *Stedman's Medical Dictionary, 26th Edition*, Williams & Wilkins, Baltimore, MD, 1995.
5. Long LR, Thoma GR. Segmentation and feature extraction of cervical spine x-ray images. Proceedings of SPIE Medical Imaging 1999: Image Processing. Vol. 3661, San Diego, CA, February 20-26, 1999, pp. 1037-1046
6. Zamora G, Sari-Sarraf H, Mitra S. Estimation of orientation of cervical vertebrae for segmentation with active shape models. Proceedings of SPIE Medical Imaging 2001: Image Processing, San Diego, CA, February 17-23, 2001 (forthcoming).
7. Long LR, Pillemer S, Goh G-H, Berman LE, Neve L,Thoma GR, Premkumar A, Ostchega Y, Lawrence R, Altman RD, Lane NE, Scott WW, Jr. A digital atlas for spinal x-rays. *Proceedings of SPIE Medical Imaging 1997: PACS Design and Evaluation: Engineering and Clinical Issues*, SPIE vol. 3035, pp. 586-594, Newport Beach, CA, February 22-28, 1997.

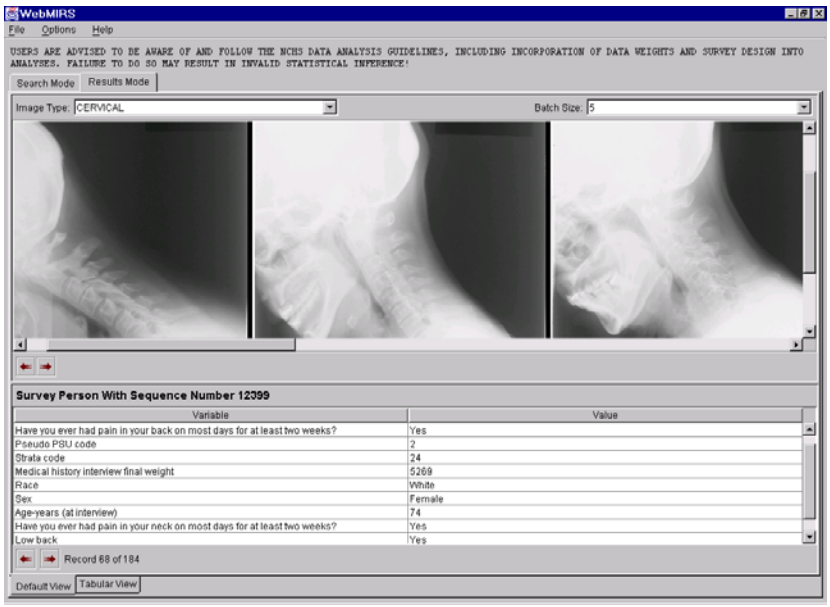

Figure 1. The WebMIRS results screen, displaying cervical spine x-rays and related text

Figure 2a. Input 1462x1755 image

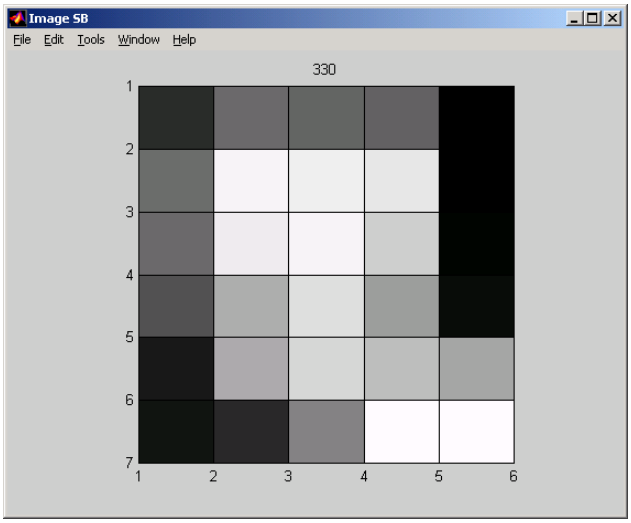

Figure 2b. Corresponding 6x7 subsampled blurred image

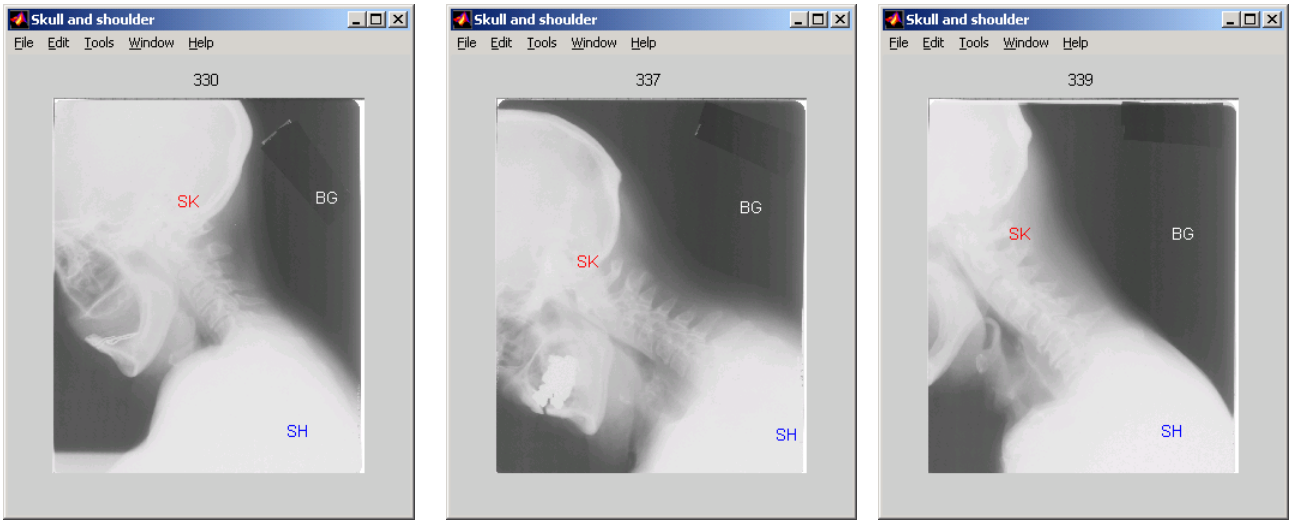

Figure 3a-c. Examples of the labeling of the landmarks obtained by analyzing the low-resolution images

Figure 4a-b. The large amount of light at the bottom of this x-ray causes the skull landmark to be misplaced. Moreover, Figure 4a shows that the skull landmark is mis-labeled "SH" when classification method (c) is used. Figure 4b shows that this landmark is correctly labeled by method (d), which first finds the "shoulder corner" of the image, and then classifies the landmark closest to this corner in Euclidean distance as the shoulder, or "SH" landmark.

Figure 5. The SH and SK landmarks (at the ends of the line segment) can be used to obtain an approximate spine axis. Points marked by squares are skull (shoulder) edge points, automatically found by analysis of the smoothed grayscale derivatives along the SH-SK line segment.

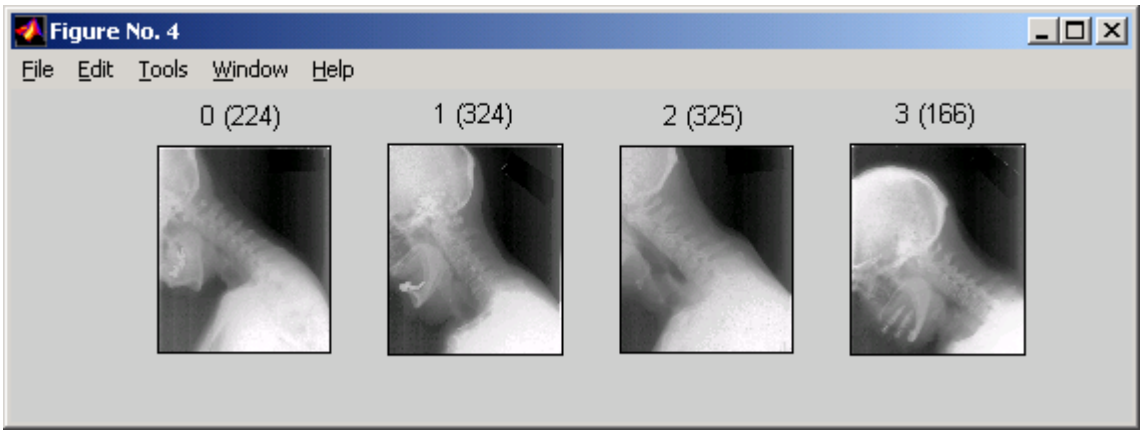

Figure 6. Cervical spine images with progressively severe anterior osteophytes (AO). Grades and image numbers are shown. Grade 0 is normal.

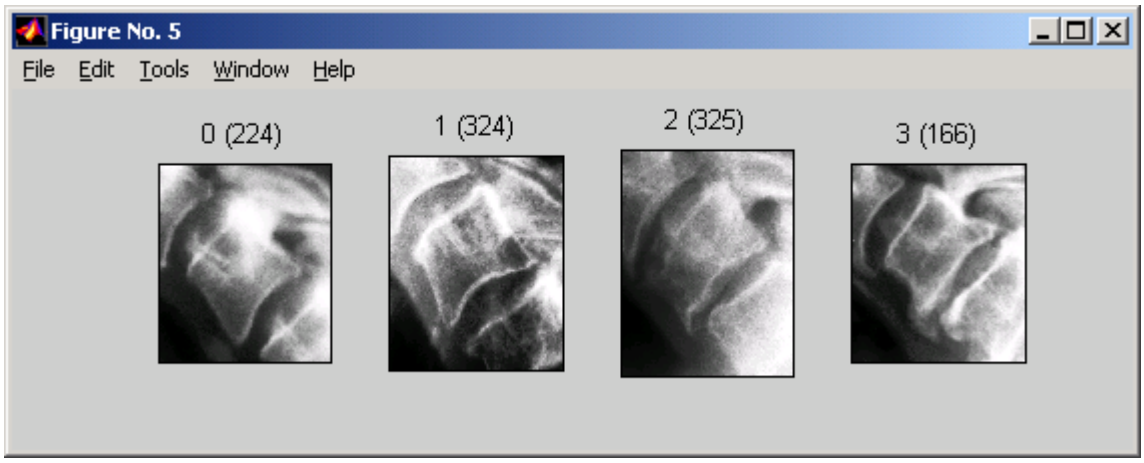

Figure 7. Vertebral regions from the Figure 6 images showing the anterior osteophytes (AO).

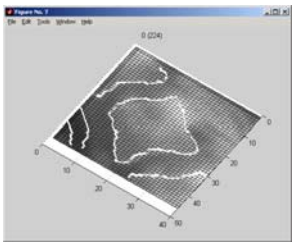

Figure 8a. AO grade 0 (normal)

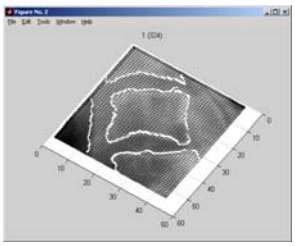

Figure 8b. AO grade 1

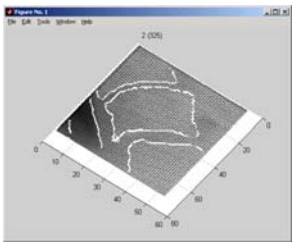

Figure 8c. AO grade 2

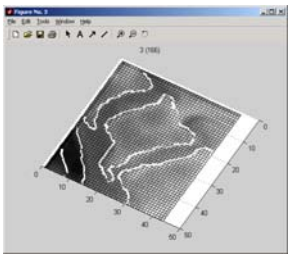

Figure 8d. AO grade3

	Skull		Shoulder		Background	
Classification Method	Accept	Reject	Accept	Reject	Accept	Reject
a	46	2	48	0	48	0
b	32	16	34	14	48	0
c	46	2	47	1	48	0
d	46	2	48	0	48	0

Table 1. Results of classification of skull, shoulder, and background landmarks for 48 cervical spine image

VID	N	NU	NL	NB
2	72	0	5	0
3	73	1	12	1
4	73	2	19	9
5	71	3	36	13
6	64	5	19	22
7	51	17	2	2

Table 2. Example of cervical spine data acquired. VID = vertebra ID (2=C2, 3=C3, etc.), N=number of images showing this vertebra, NU=number of images with AO at upper corner only of this vertebra, NL=number of images with AO at lower corner only of this vertebra, NB=number of images with AO at both upper and lower corners of this vertebra